International Symposium on Information Theory and its Applications, ISITA2004
Parma, Italy, October 10–13, 2004

Tight Bounds on the SER and BER of Space-Time Orthogonal Block Coded Channels under MAP Decoding

Firouz Behnamfar†, Fady Alajaji†‡, and Tamás Linder†‡

† Department of Electrical and Computer Engineering
‡ Department of Mathematics and Statistics
Queen's University, Kingston
Ontario K7L 3N6, Canada
E-mail: {firouz, fady, linder}@mast.queensu.ca

Abstract

We study the maximum *a posteriori* (MAP) decoding of space-time orthogonal block coded memoryless non-uniform sources transmitted over multiple input-multiple output channels with flat Rayleigh fading. We use the pairwise error probability and the probability of the intersection of two pairwise error events to establish tight algorithmic Bonferonni-type upper and lower bounds on the symbol error rate (SER) and bit error rate of PSK and QAM signaling schemes under MAP decoding. The problem of mapping the binary sequence to the constellation points is also studied. It is shown that for a binary source with $P(X = 0) = 0.9$ and with 64-QAM signaling and MAP decoding, a judiciously constructed mapping can achieve a channel signal-to-noise ratio (CSNR) gain of 3.64 dB over Gray-type mappings at SER $= 10^{-3}$. The advantage of MAP decoding over separate (tandem) source and channel coding is also explored.

1. INTRODUCTION

The original papers published on space-time trellis codes and space-time orthogonal block (STOB) codes [11] adopt the Chernoff upper bound to estimate the pairwise error probability of codewords and build code design criteria. Although the Chernoff bound results in successful code constructions, it is quite loose even at high values of the channel signal-to-noise ratio (CSNR). It is common practice in the literature to use the union bound to approximate the system SER. However, the union bound is intrinsically loose particularly at low CSNR. Therefore, using the Chernoff bound together with the union bound results in poor approximations to system performance. In [4], an exact closed form expression for the pairwise error probability (PEP) of MAP-decoded STOB codes was derived and it was shown that the PEP can be significantly lower under MAP decoding as compared with ML decoding for strongly non-uniform memoryless sources.

MAP decoding for sources with non-uniform distribution and/or memory is a form of joint source-channel coding. Most previous coding designs, such as the work in [2, 9], show that independent (tandem) source and channel coding outperforms joint source-channel coding above some threshold CSNR. An opposite behavior is however observed in [14], where joint source-channel coding based on Turbo coding (with significantly longer block lengths) outperforms tandem coding. As can be seen in the simulations of this paper, the CSNR threshold beyond which tandem coding outperforms MAP decoding is large. In particular, there are many examples in which joint source-channel coding outperforms tandem coding for the entire CSNR range of interest. Indeed, in an information theoretic study [13], it is proved that the error exponent (which is the rate of asymptotic exponential decay of the probability of block error) of optimal joint source-channel coding can be as large as twice the error exponent of optimal tandem systems, which concatenate optimal source coding with optimal channel coding. This implies that for the same probability of error, optimal joint source-channel coding would require *half* the encoding/decoding delay of the optimal tandem scheme.

In this paper, we establish very tight algorithmic Bonferonni-type upper and lower bounds on the SER and BER of STOB coded channels under MAP decoding. The bounds are very close and often coincide up to four significant digits even at moderate CSNR values. We also employ the results of [10] to study how mapping from the binary bit-sequence (input to the modulator) to the constellation points can improve the symbol and bit error performance of STOB coded chan-

This work was supported in part by the Natural Sciences and Engineering Research Council (NSERC) of Canada and the Premier's Research Excellence Award (PREA) of Ontario.

nels.

2. SYSTEM MODEL

The multiple input-multiple output (MIMO) communication system considered here employs K transmit and L receive antennas. The input to the system is an i.i.d. bit-stream which can have non-uniform distribution. The baseband constellation points are denoted by $\{c_{(k)}\}_{k=1}^{2^p}$ where p is a positive integer. We will assume that $E\{|c_{(k)}|^2\} = 1$. At symbol period t, the signals $\{s_t^i\}_{i=1}^K$ are simultaneously transmitted (see below). The channel is assumed to be Rayleigh flat fading, so that the complex path gain from transmit antenna i to receive antenna j, denoted by H_{ji}, has a zero-mean unit-variance complex Gaussian distribution, denoted by $\mathcal{CN}(0,1)$, with i.i.d. real and imaginary parts. We assume that the receiver, but not the transmitter, has perfect knowledge of the path gains. Moreover, we assume that the channel is quasi-static, meaning that the path gains remain unchanged during a codeword transmission, but vary in an i.i.d. fashion from one codeword interval to the other. The additive noise at receiver j at time t, N_t^j, is assumed to be $\mathcal{CN}(0,1)$ distributed with i.i.d. real and imaginary parts. We finally assume that the input, fading coefficients, and channel noise are independent from each other. Based on the above, for a CSNR of γ_s at each receive branch and at time t, the signal at receive antenna j can be written as

$$R_t^j = \sqrt{\frac{\gamma_s}{K}} \sum_{i=1}^{K} H_{ji} s_t^i + N_t^j.$$

Let $\mathbf{c} = (c_1, ..., c_\tau)^T$ be a vector of τ consecutive constellation points and $\mathbf{S} = (\mathbf{s}_1, ..., \mathbf{s}_w)$ be the space-time code corresponding to it, where w is the codeword length, $\mathbf{s}_t = (s_t^1, ..., s_t^K)^T$, and ^{T} denotes transposition. In the case of STOB codes, we have $w = g\tau$, where g is the coding gain and $\mathbf{S}\mathbf{S}^\dagger = g\|\mathbf{c}\|^2 \mathbf{I}_\tau$, where $\mathbf{I}_\tau$ is the $\tau \times \tau$ identity matrix and † represents complex conjugate transposition. As an example, for the code $\mathcal{G}^3$ in [11], $w = 8$, $\tau = 4$, and $g = 2$, and for Alamouti's $\mathcal{G}^2$ code [3], $g = 1$ and $w = \tau = 2$. The input-output relationship of STOB coded channels can be written as [4]

$$\tilde{\boldsymbol{r}}^j = g\sqrt{\frac{\gamma_s}{K}} Y_j \mathbf{c} + \tilde{\boldsymbol{n}}^j,$$

where $Y_j = \sum_i |H_{ji}|^2$ and $\tilde{\boldsymbol{n}}^j = (\tilde{N}_1^j, ..., \tilde{N}_\tau^j)^T$ is an additive white Gaussian noise vector with i.i.d. components of distribution $\tilde{N}_t^j \sim \mathcal{N}(0, gY_j)$.

3. SER AND BER BOUNDS UNDER MAP DECODING

In this section, we derive the formulas to compute Bonferroni-type upper and lower bounds on the SER and BER of space-time orthogonal block coded channels under MAP decoding. Two computationally less demanding bounds on the BER are also presented in Subsection 4.2.

For a positive integer M, let $A_1, ..., A_M$ be events in an arbitrary probability space. A stepwise algorithm is proposed in [8] to compute the following Bonferroni-type lower bound, due to Kounias [7], for the probability of the union of the A_i:

$$P\left(\bigcup_{i=1}^{M} A_i\right) \geq \max_{\mathcal{I}} \left\{ \sum_{i\in\mathcal{I}} P(A_i) - \sum_{\substack{i,j\in\mathcal{I}\\ i<j}} P(A_i \cap A_j) \right\}, \tag{1}$$

where $\mathcal{I} \subseteq \{1, 2, ..., M\}$. Also, as shown in [8], one can employ Kruskal's greedy algorithm [1] to calculate the Hunter [5] Bonferroni-type upper bound for the probability of the union of the A_i, which is given by

$$P\left(\bigcup_{i=1}^{M} A_i\right) \leq \sum_{i=1}^{M} P(A_i) - \max_{T_0\in\mathcal{T}} \sum_{(i,j)\in T_0} P(A_i \cap A_j), \tag{2}$$

where $\mathcal{T}$ is the set of all spanning trees of the M indices, i.e., the trees that include all indices as nodes.

3.1. The Symbol Error Rate

For a constellation of size M, the SER under symbol MAP decoding is given by

$$\begin{aligned}\text{SER} &= \sum_{u=1}^{M} P\left(\epsilon | c_{(u)}\right) p\left(c_{(u)}\right) \\ &= \sum_{u=1}^{M} P_u \left(\bigcup_{i\neq u} \epsilon_{ui}\right) p(u), \end{aligned} \tag{3}$$

where $p(u) \triangleq p(c_u)$, $P\left(\cdot | c_{(u)}\right) \triangleq P_u(\cdot)$ is the conditional probability given that $c_{(u)}$ was sent, and ϵ_{ui} indicates the error event that $c_{(i)}$ has a larger MAP metric than $c_{(u)}$ (i.e., $c_{(i)}$ is preferred to $c_{(u)}$ at the receiver). To find lower and upper bounds on the probability of each union in (3), we need to find the probability of ϵ_{ui} and its intersection with ϵ_{uj}, which we will refer to as the 2-D PEP of $c_{(u)}$ with $c_{(i)}$ and $c_{(j)}$. We note that $P_u(\epsilon_{ui})$ is indeed the PEP. It was shown in [4] that the PEP between symbols $c_{(u)}$ and $c_{(i)}$ is given in (4), where

$$P_u(\epsilon_{ui}) = \frac{1-\mathrm{sgn}(\lambda_{ui})}{2} - \frac{1}{2}e^{-\left(\lambda_{ui}+|\lambda_{ui}|\sqrt{2\delta_{ui}^{-2}+1}\right)}$$
$$\times \sum_{k=0}^{n-1}\left\{\frac{(-1)^{n+k-1}}{(\delta_{ui}^2+2)^{n-k-1}}\left(-\mathrm{sgn}(\lambda_{ui}) + \frac{\delta_{ui}}{\sqrt{\delta_{ui}^2+2}}\sum_{m=0}^{k}\binom{2m}{m}\frac{1}{(2\delta_{ui}^2+4)^m}\right)\sum_{l=1}^{n-k-1}\alpha_{n,k}^l\frac{|\lambda_{ui}|^l(\delta_{ui}^2+2)^{l/2}}{l!\delta_{ui}^l}\right\} \quad (4)$$

$$\delta_{ui}^2 = \frac{g\gamma_s}{2K}|c_{(u)}-c_{(i)}|^2, \quad \lambda_{ui} = \frac{1}{2}\ln\{p(u)/p(i)\},$$

$\mathrm{sgn}(x) = |x|/x$ if $x \neq 0$ and 0 otherwise,

$$\alpha_{n,k}^l = \sum_{m=0}^{l-1}\binom{l}{m}(-1)^{l+m}\prod_{q=0}^{n-k-2}(l-m-2q),$$

and we have set $\sum_{i=L}^{U}\beta_i = 1$ for $L > U$. We can also show that the 2-D PEP may be found via

$$P_u(\epsilon_{ui}\cap\epsilon_{uj}) =$$
$$E_Y\left\{\Psi\left(\rho_{iju}, \delta_{ui}\sqrt{Y}+\frac{\lambda_{ui}}{\delta_{ui}\sqrt{Y}}, \delta_{uj}\sqrt{Y}+\frac{\lambda_{uj}}{\delta_{uj}\sqrt{Y}}\right)\right\},$$

where $Y = \sum_{i,j}|H_{ji}|^2$,

$$\rho_{iju} = \frac{\langle c_{(i)}-c_{(u)}, c_{(j)}-c_{(u)}\rangle}{|c_{(u)}-c_{(i)}||c_{(u)}-c_{(j)}|},$$

and

$$\Psi(\rho,a,b) = \frac{1}{2\pi\sqrt{1-\rho^2}}\int_a^\infty\int_b^\infty e^{-\frac{\tau^2-2\rho\tau\lambda+\lambda^2}{2(1-\rho^2)}}d\tau d\lambda \quad (5)$$

is the bivariate Gaussian function.

3.2. The Bit Error Rate

Under symbol MAP decoding, the BER is given by

$$\mathrm{BER} = \sum_{u=1}^{M}p(u)P_b(u), \quad (6)$$

where $P_b(u)$ is the bit error probability given that $c_{(u)}$ is sent. Noting that $P\left(\hat{c}=c_{(j)}|c=c_{(u)}\right) = \left(1-P_u\left(\bigcup_{i\neq j}\epsilon_{ij}\right)\right)$, we have

$$P_b(u) = \frac{1}{\log_2 M}\sum_{j=1}^{M}D_H(j,u)\left(1-P_u\left(\bigcup_{i\neq j}\epsilon_{ij}\right)\right), \quad (7)$$

where $D_H(j,u)$ is the Hamming distance between the bit assignments of $c_{(j)}$ and $c_{(u)}$. From the above, it is clear that finding the upper and lower bounds on the BER requires the evaluation of lower and upper bounds on the probability of the union in (7), respectively. These bounds, in turn, require the computation of

$$P_u(\epsilon_{ij}) = E_Y\left\{Q\left(\frac{\delta_{ui}^2-\delta_{uj}^2}{\delta_{ij}}\sqrt{Y}+\frac{\lambda_{ij}}{\delta_{ij}\sqrt{Y}}\right)\right\},$$

and $P_u(\epsilon_{ij}\cap\epsilon_{kj})$, which is the expected value of

$$\Psi\left(\rho_{ikj}, \Delta_{u,ij}^2\sqrt{Y}+\frac{\lambda_{ij}}{\delta_{ij}\sqrt{Y}}, \Delta_{u,kj}^2\sqrt{Y}+\frac{\lambda_{kj}}{\delta_{kj}\sqrt{Y}}\right)$$

with respect to Y, where $\Delta_{u,ij}^2 = (\delta_{ui}^2-\delta_{uj}^2)/\delta_{ij}$. Therefore, the results of Section 3.1 can be used here to compute the lower and upper bounds on the BER.

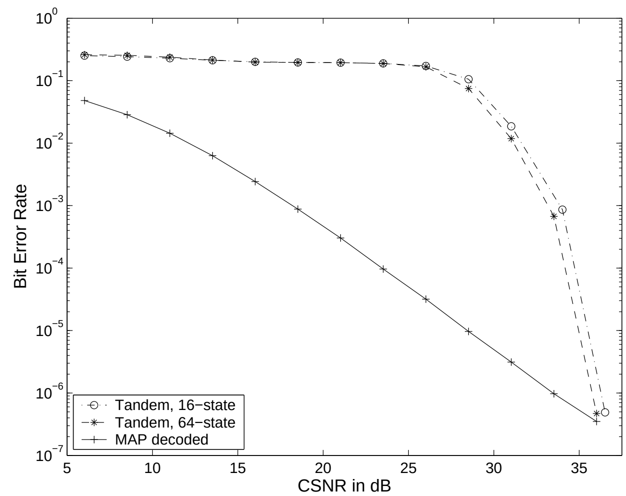

Figure 1: Comparison between tandem and MAP-decoded 16-QAM schemes with Gray mapping for a system with $K=2$, $L=1$, and $\mathcal{G}^2$ STOB code.

4. NUMERICAL RESULTS

4.1. Tandem vs. Joint Source-Channel Coding

Figure 1 compares a MAP decoded system with two tandem systems for a dual transmit-single receive MIMO channel with $\mathcal{G}^2$ code, 16-QAM signaling,

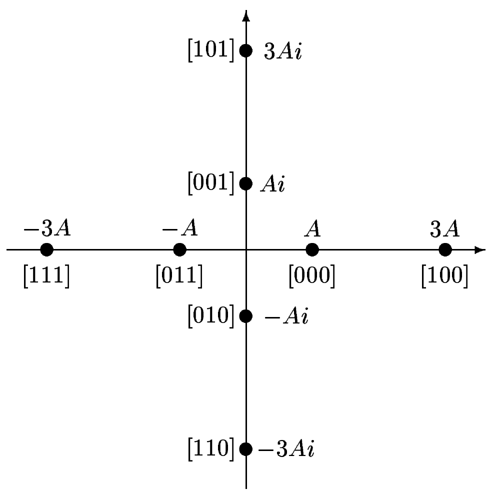

Figure 2: The star-QAM signaling scheme with quasi-Gray mapping. A is a normalizing factor and equals $1/2\sqrt{10}$ and $i = \sqrt{-1}$.

and Gray mapping. The input is an i.i.d. bit-stream with $P(X = 0) = 0.89$ so that the source entropy is $H(X) = 0.5$. The tandem systems comprise Huffman coding of order 4 followed by 16-state or 64-state rate-1/2 convolutional coding. The convolutional codes are non-systematic and are the best codes reported in [6] in terms of having the largest free distance. The length of the input bit-stream is two million bits. The test is repeated 1000 times and the average BER is reported. For MAP decoding, ten million bits are used.

It is observed that the MAP-decoded system is superior to the tandem system when the BER is larger than 10^{-6}, which is the BER range of interest in many applications. We have also observed that as the constellation size increases, the MAP decoded system is superior for a wider range of the CSNR. Note that the memory and computational complexity of the tandem system considered here is significantly higher than the MAP-decoded system.

4.2. SER and BER Bounds for M-ary Signaling

In this subsection we study the SER and BER bounds and the simulation results for i.i.d. inputs with two dimensional signaling for a dual transmit-single receive system. Two systems are considered: one with an equiprobable input and ML decoding and another with $P(X = 0) = 0.9$ and MAP decoding. For SER, the union bound given by

$$\text{Union Bound} = \sum_u p(u) \sum_i P_u(\epsilon_{ui})$$

is also plotted. To have an estimate of the BER, one

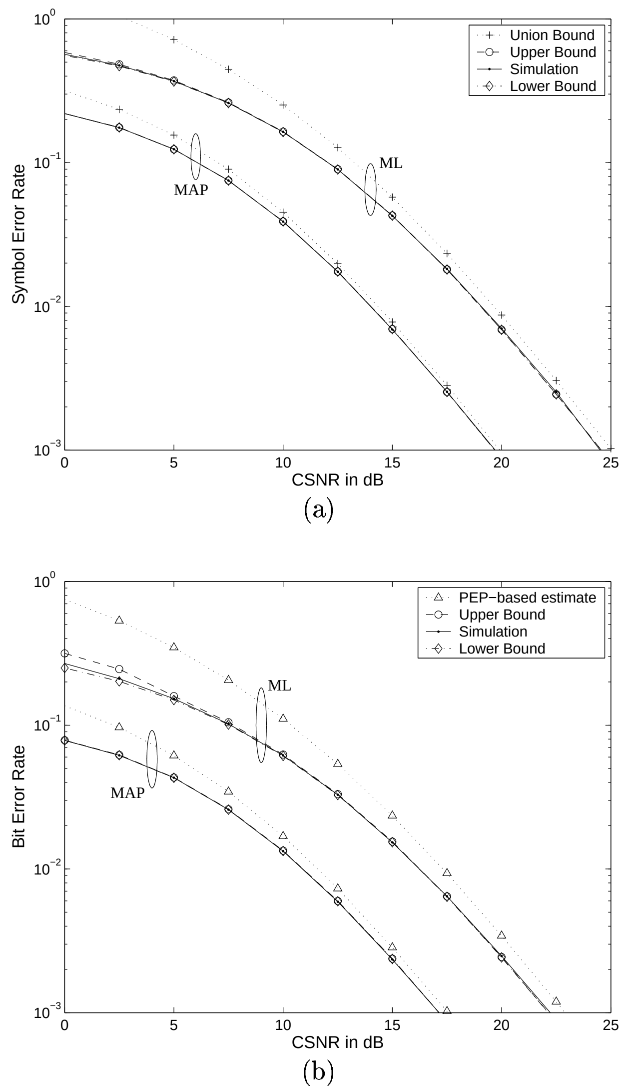

Figure 3: (a) SER and (b) BER curves for 8-Point Star QAM modulation with quasi-Gray mapping, $K = 2$, $L = 1$, and $\mathcal{G}^2$ STOB code.

can replace $P\left(\hat{c} = c_{(j)} | c = c_{(u)}\right)$ with $P_u(\epsilon_{uj})$ in (7). This will result in an upper bound on the BER, because $P_u(\epsilon_{uj}) \geq P\left(\hat{c} = c_{(j)} | c = c_{(u)}\right)$. Since Gray mapping is used, $\text{SER}/\log_2(M)$ is plotted as a lower bound on the BER.

In order to emphasize the fact that the bounding technique presented in this paper puts no constraints on the signaling or mapping schemes, we consider a non-standard (neither PSK nor square-QAM) 8-point Star-QAM signaling scheme in Figure 2, where a quasi-Gray signal mapping is indicated in brackets. The SER and BER curves of this scheme are plotted in Figures 3.a and 3.b, respectively, and demonstrate the tightness of the bounds. Note that the bounds become tighter

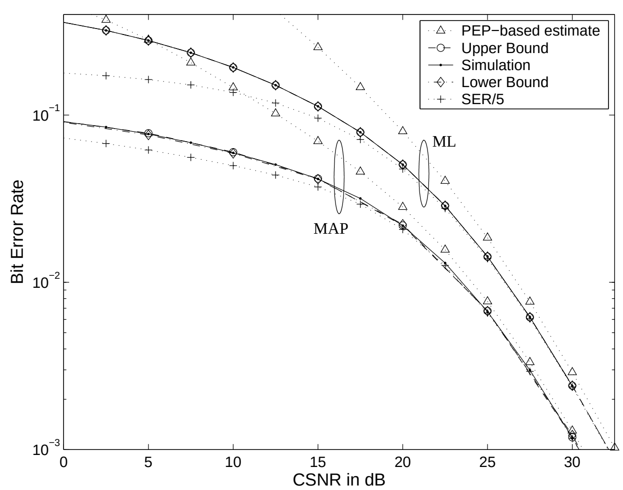

Figure 4: BER curves for 32-PSK modulation with Gray mapping for a system with $K = 2$, $L = 1$, and $\mathcal{G}^2$ STOB code.

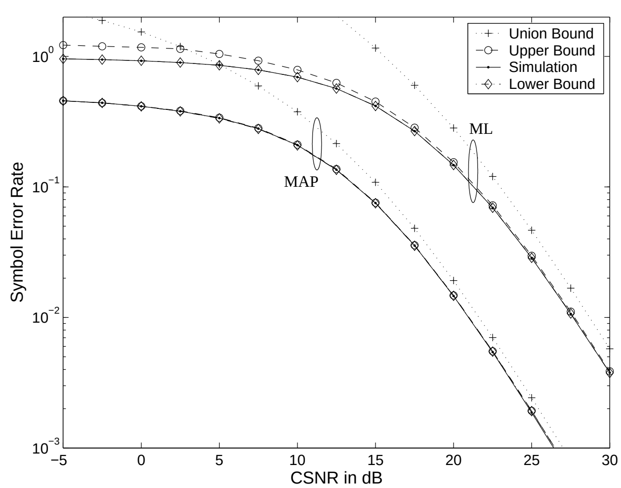

Figure 5: SER curves for 64-QAM modulation with Gray mapping for a system with $K = 2$, $L = 1$, and $\mathcal{G}^2$ STOB code.

as the source becomes more biased.

We observe from Figure 4 that the BER bounds provide an excellent approximation even for negative CSNR values and large constellations such as 32-PSK. This figure also shows that the PEP-based BER estimate is often very loose (as compared with the other bounds). The gain of MAP decoding over ML decoding is 1.85 dB at BER $= 10^{-3}$. Figure 5 presents the SER curves for 64-QAM and Gray mapping. It is interesting to note again that as the source becomes more biased, the bounds become tighter (this is specially true for the upper bound). The curves also show that, as expected, the union bound becomes looser as the CSNR decreases. The MAP decoding gain at SER $= 10^{-3}$ is as

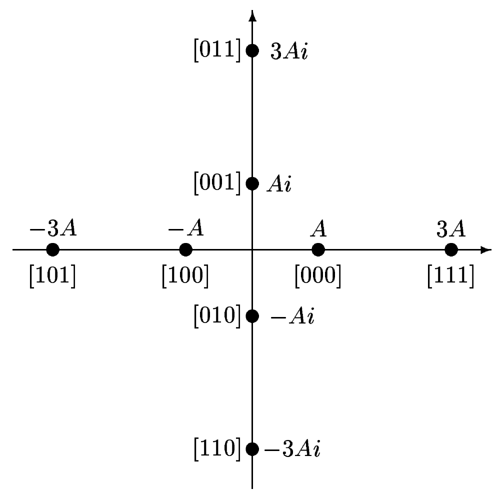

Figure 6: The star-QAM signaling scheme with M1 mapping.

large as 6.7 dB. The upper bound for the ML-decoded system is up to 10% larger than the lower bound at low CSNR values, but it becomes tight as the CSNR grows. Both bounds are tight for the MAP-decoded case.

Further tests show that the bounds are tighter for smaller constellations and they are as tight for other values of $P(X = 0)$.

4.3. The Effect of Constellation Mapping

We next demonstrate that a large gain can be achieved via signal mappings designed according to the source non-uniform distribution over Gray and quasi-Gray mappings. The M1 mapping was introduced in [10] and was designed for the transmission of non-uniform binary sources over single antenna additive white Gaussian noise channels. It was shown in [12] that the M1 map minimizes the SER union bound for single antenna Rayleigh fading channels with M-ary PSK and square QAM signaling.

Based on the design criteria proposed in [10], we construct an M1-type signal mapping for the star-QAM signaling scheme as shown in Figure 6. The SER performance of the M1 and quasi-static mappings are compared in Figure 7. It is observed that even for this small signaling scheme, the CSNR gain of M1 mapping over quasi-Gray mapping is nearly 2 dB with MAP decoding at SER $= 10^{-3}$. The gain due to source redundancy when the source distribution varies between 0.5 to 0.9 is 7 dB with M1 mapping. Figure 8 compares the SER curves for the Gray and M1 mappings for 64-QAM signaling. This figure shows that the M1 map performs very well for MIMO channels. The gain of the M1 mapping over Gray mapping is 3.7 dB at SER $= 10^{-3}$. The gain due to source redundancy is 10.4 dB.

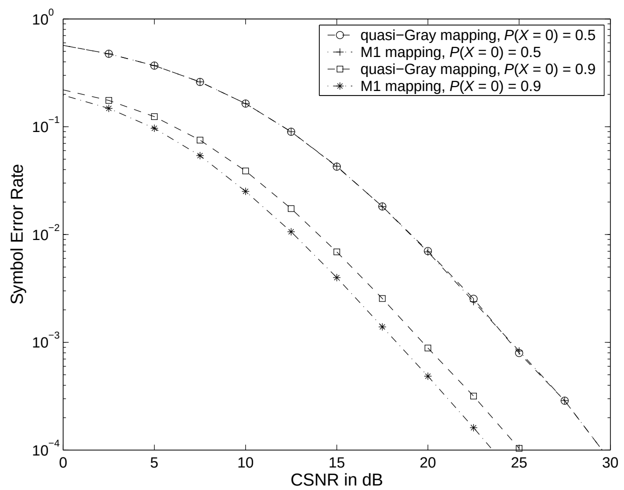

Figure 7: Comparison between the quasi-Gray and the M1 mappings with Star QAM for a system with $K = 2$, $L = 1$, and $\mathcal{G}^2$ STOB code.

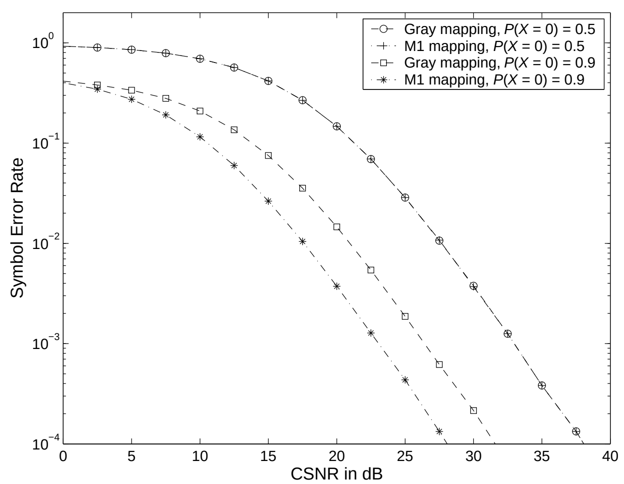

Figure 8: Comparison between the Gray and the M1 mappings with 64-QAM for a system with $K = 2$, $L = 1$, and $\mathcal{G}^2$ STOB code.

References

[1] R. K. Ahuja, T. L. Magnanti, and J. B. Orlin, *Network Flows.* Englewood Cliffs, NJ: Prentice Hall, 1993.

[2] F. Alajaji, N. Phamdo, N. Farvardin, and T. Fuja, "Detection of binary Markov sources over channels with additive Markov noise," *IEEE Trans. Inform. Theory,* vol. 42, pp. 230-239, Jan. 1996.

[3] S. M. Alamouti, "A simple transmitter diversity scheme for wireless communications," *IEEE J. Select. Areas Commun.*, vol. 16, pp. 1451-1458, Oct. 1998.

[4] F. Behnamfar, F. Alajaji, and T. Linder, "Performance analysis of MAP decoded space-time orthogonal block codes for non-uniform sources," in *Proc. IEEE Inform. Theory Workshop*, Paris, France, pp. 46-49, Mar.-Apr. 2003.

[5] D. Hunter, "An upper bound for the probability of a union," *J. Appl. Probab.*, vol. 13, pp. 597-603, 1976.

[6] R. Johannesson and K. Zigangirov, *Fundamentals of Convolutional Coding.* New York, NY: IEEE Press, 1999.

[7] E. G. Kounias, "Bounds on the probability of a union, with applications," *Ann. Math. Statist.*, vol. 39, pp. 2154-2158, 1968.

[8] H. Kuai, F. Alajaji, and G. Takahara, "Tight error bounds for nonuniform signaling over AWGN channels," *IEEE Trans. Inform. Theory*, vol. 46, pp. 2712-2718, Nov. 2000.

[9] J. Lim and D. L. Neuhoff, "Joint and tandem source-channel coding with complexity and delay constraints," *IEEE Trans. Commun.*, vol. 51, pp. 757-766, May 2003.

[10] G. Takahara, F. Alajaji, N. C. Beaulieu and H. Kuai, "Constellation mappings for two-dimensional signaling of non-uniform sources," *IEEE Trans. Commun.*, vol. 51, pp. 400-408, Mar. 2003.

[11] V. Tarokh, H. Jafarkhani, and A. R. Calderbank, "Space-time block codes from orthogonal designs," *IEEE Trans. Inform. Theory*, vol. 45, pp. 1456-1467, July 1999.

[12] L. Zhong, F. Alajaji, and G. Takahara, "Error analysis for non-uniform signaling over Rayleigh fading channels," submitted to *IEEE Trans. Commun.*, 2003.

[13] Y. Zhong, F. Alajaji, and L. Campbell, "When is joint source-channel coding worthwhile: an information theoretic perspective," in *Proc. 22^{nd} Biennial Symp. Commun.*, Kingston, ON, June 2004.

[14] G.-C. Zhu, F. Alajaji, J. Bajcsy and P. Mitran, "Transmission of non-uniform memoryless sources via non-systematic turbo codes," *IEEE Trans. Commun.*, vol. 52, Aug. 2004.